Scattering Length Instability in Dipolar Bose-Einstein Condensates

D. C. E. Bortolotti,[1,2] S. Ronen,[1] J. L. Bohn,[1] and D. Blume[3]

[1]JILA, NIST and Department of Physics, University of Colorado, Boulder, Colorado 80309-0440, USA
[2]LENS and Dipartimento di Fisica, Universitá di Firenze, and INFM, Sesto Fiorentino, Italy
[3]Department of Physics and Astronomy, Washington State University, Pullman, Washington 99164-2814, USA

(Received 18 April 2006; published 18 October 2006)

We predict a new kind of instability in a Bose-Einstein condensate composed of dipolar particles. Namely, a comparatively weak dipole moment can produce a large, negative two-body scattering length that can collapse the Bose-Einstein condensate. To verify this effect, we validate mean-field solutions to this problem using exact, diffusion Monte Carlo methods. We show that the diffusion Monte Carlo energies are reproduced accurately within a mean-field framework if the variation of the s-wave scattering length with the dipole strength is accounted for properly.

DOI: 10.1103/PhysRevLett.97.160402 PACS numbers: 03.75.Nt

The recently achieved Bose-Einstein condensation of atomic chromium [1,2] has added two new twists to the study of ultracold matter. First, Cr condensates realize the first spin-three spinor condensate [3,4]. Second, they exhibit, due to Cr's comparatively large magnetic dipole moment, observable anisotropic long-range interactions [5]. These long-range interactions allow the relative orientation between well separated atoms or molecules to be controlled, either by tuning external fields or else by adjusting trap anisotropy. An extensive theoretical literature has predicted novel properties for these gases. For example, rotonlike features have been predicted for trapped gases [6,7], along with unique phases such as checkerboard and supersolid phases [8–10].

Rapid experimental progress in cooling and trapping suggests that condensation of ground state molecules with large permanent dipole moments, such as OH [11,12], RbCs [13], KRb [14], and NH [15], may be achieved soon. These species would represent truly strongly interacting dipoles, with interparticle interaction strengths up to $\sim 10^3$ times larger than in chromium. Indeed, the dipolar interactions could become the dominant energy scale in such systems, driving transitions to correlated states of these gases.

Thus far, dipolar Bose gases at zero temperature have been described using an approximate mean-field, Gross-Pitaevskii (GP) description, which has proven adequate to describe experiments in Cr [5]. Stability diagrams and excitation spectra have been derived within this formalism [16–24]. Somewhat surprisingly, the validity of the GP equation for dipolar gases with strong, anisotropic long-range interactions has not been assessed in detail to date. *Per se,* it is not clear that a Hartree wave function, as used in the GP framework, can properly describe systems interacting through potentials that fall off as $\pm 1/r^3$ at large interparticle distances. Neutral atom-atom interactions, e.g., fall off as $-1/r^6$ and mean-field treatments are shown to predict the properties of dilute atomic Bose gases with high accuracy. This requires, however, replacing the true interaction by an appropriate Fermi pseudopotential. For electronic systems with repulsive $1/r$ interactions, a Hartree-Fock formalism is a suitable starting point for computing the electronic structure of atoms and molecules. An accurate determination of observables, however, often requires correlation effects beyond those described by a Hartree-Fock wave function.

Because the applicability of the GP equation is completely unknown for dipolar interactions, we undertake here its verification. We report essentially exact many-body diffusion Monte Carlo (DMC) calculations for dipolar Bose gases interacting through realistic two-body model potentials. The results reveal that the GP equation is adequate to describe the gas, *provided* that the pseudopotential is parametrized in terms of a "dipole-dependent" s-wave scattering length $a(d)$ as anticipated in Ref. [17] [and provided, as usual, that $na(d)^3 \ll 1$]. A main finding of this Letter is that the variation of scattering length with dipole moment plays a vital role in the stability of the gas against macroscopic collapse. Even if the dipole-dipole interaction itself is not strong enough to instigate collapse, nevertheless the dipole-dependent scattering length may become sufficiently negative to do so.

Consider the Hamiltonian H for N interacting bosonic dipoles with mass m, assumed to be polarized along the z axis, under external harmonic confinement,

$$H = \sum_{j=1}^{N}\left(\frac{-\hbar^2}{2m}\nabla_j^2 + \frac{1}{2}m\omega^2\vec{r}_j^{\,2}\right) + \sum_{j<k}^{N} V(\vec{r}_{jk}), \qquad (1)$$

where ω denotes the trapping frequency, $\vec{r}_j$ the position vector with respect to the trap center of the jth dipole, and $\vec{r}_{jk}$ the distance vector $\vec{r}_{jk} = \vec{r}_j - \vec{r}_k$. We model the boson-boson potential $V(\vec{r})$ by a short-range hard core with cutoff radius b and a long-range tail with dipole moment d,

$$V(\vec{r}) = \begin{cases} d^2\frac{1-3\cos^2\theta}{r^3} & \text{if } r \geq b, \\ \infty & \text{if } r < b, \end{cases} \qquad (2)$$

where θ denotes the angle between the vector $\vec{r}$ and the

laboratory z axis. The length $D_* = md^2/\hbar^2$, at which the characteristic two-body potential and kinetic energies coincide, is used in the following to characterize the anisotropic long-range interaction.

The Hamiltonian H in Eq. (1) applies, in cgs units, to bosons with either magnetic or electric dipole moments. Importantly, the induced dipole moments that drive the interaction can be tuned in either case [25]. Consequently, the ratio D_*/b, and hence the relative importance of the dipolar interaction compared to the short-range interaction, can be changed essentially at will. This motivates us to investigate the zero temperature equilibrium properties of dipolar Bose gases over a wide range of D_*/b, including the short-range dominated regime with $D_*/b \ll 1$ and the long-range dominated regime with $D_*/b \gg 1$. Note that, to date, the effects of dipolar interactions have been observed experimentally only for atomic Cr with $D_*/b \approx 0.4$ (taking b to be the s-wave scattering length).

We start our discussion by considering two interacting dipoles, $N = 2$. After separating off the center of mass part of H, we rewrite the Hamiltonian for the relative coordinate in spherical coordinates and solve the corresponding two-dimensional Schrödinger equation numerically using standard techniques. We first determine scattering and bound state solutions in the absence of an external confining potential, i.e., for $\omega = 0$. Figure 1(a) shows the zero-energy s-wave scattering length a as a function of D_*/b. We refer to a calculated for $d^2 = 0$ as the "bare" scattering length and to a calculated for finite d^2 as the "dipole-dependent" scattering length. For $D_* = 0$, no two-body bound states exist and a is equal to b. The scattering length a decreases with increasing D_* and diverges and changes sign at $D_*/b \approx 8.5$, signaling the creation of a two-body bound state. At $D_*/b \approx 19$, a shows a second divergence corresponding to a second s-wave bound state being pulled in.

Trapped two-body systems could be prepared experimentally by loading ultracold polar molecules into a very deep optical lattice and realizing doubly occupied lattice sites. To determine the energy spectrum of two trapped dipoles, we fix the short-range two-body length b, i.e., $b = 0.0137a_{\mathrm{ho}}$, and vary D_*/a_{ho}, where a_{ho} denotes the oscillator length $a_{\mathrm{ho}} = \sqrt{\hbar/(m\omega)}$. The dashed lines in Fig. 1(b) show the total energy E/N per dipole as a function of D_*/a_{ho}. Comparison of Figs. 1(a) and 1(b) reveals that the energetically lowest-lying state with positive energy becomes negative at about the same value of D_* as that for which the scattering length a diverges [the D_* values shown in Figs. 1(a) and 1(b) extend, although scaled differently, over the same range]. Furthermore, the trap energies nearly coincide with those for a noninteracting two-particle gas, i.e., $E/N = 1.5, 2.5, \ldots, \hbar\omega$, at D_* values for which $a = 0$. The s-wave scattering length, which depends only on the ratio D_*/b, thus determines the gross features of the energy level spectrum of two interacting dipoles under external spherical confinement. The details of the energy spectrum, however, depend additionally on the magnitude of D_* or b.

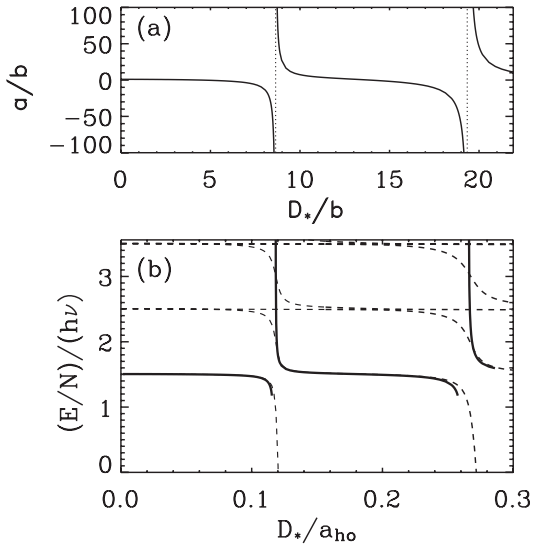

FIG. 1. (a) Solid lines show the s-wave scattering length a as a function of the dipole strength D_*, both in units of b, for the two-body potential V, Eq. (2). Vertical dotted lines denote those D_*/b values at which a diverges and a new bound state appears in the two-body potential. (b) Dashed lines show E/N for two dipoles under external spherical confinement calculated for $b = 0.0137a_{\mathrm{ho}}$ as a function of D_*/a_{ho} obtained by solving the linear Schrödinger equation for the Hamiltonian given by Eq. (1). Solid lines show the corresponding GP energy obtained by solving Eq. (4) for the pseudopotential V_{eff}, Eq. (3), using the dipole-dependent scattering length. The GP energies are plotted for each branch of the two-body spectrum. Note that the D_* values shown in (a) and (b) extend over the same range.

For $N > 2$, we solve the Schrödinger equation using the DMC technique with importance sampling, which determines the ground state energy of the time-independent Schrödinger equation by propagating an initial "walker distribution" in imaginary time and projecting out the lowest stationary eigenstate [26]. To efficiently treat large systems, a stochastic realization of the short-time Green's function propagator is used, which introduces a statistical uncertainty of any DMC expectation value. Details of the procedure will be presented elsewhere [27]. The symbols in Fig. 2 show our DMC energies E/N per dipole for $b = 0.0137a_{\mathrm{ho}}$ (and d^2 values for which V supports no two-body bound states) as a function of D_*/a_{ho} for $N = 4$, 10, 20, and 50. Statistical uncertainties are indicated by vertical error bars. For completeness, the dashed lines show the E/N data for $N = 2$ from Fig. 1(b). The energy E/N per dipole decreases with increasing D_*. In particular, E/N becomes smaller than the ideal gas value of $1.5\hbar\omega$ for negative s-wave scattering lengths (D_*/a_{ho} greater than ≈ 0.06 in the figure). Finally, for fixed D_*/a_{ho}, the attractive part of the dipolar interaction leads to a decrease of E/N with increasing N. We find qualitatively similar be-

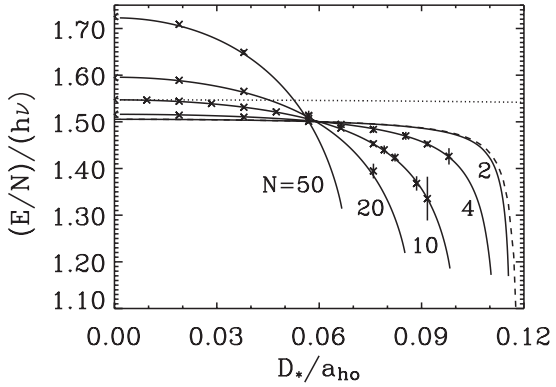

FIG. 2. Symbols show the energy per particle E/N calculated by the DMC method for $b = 0.0137a_{\mathrm{ho}}$ as a function of D_*/a_{ho} for $N = 4$, 10, 20, and 50. Vertical error bars indicate statistical uncertainties. For completeness, a dashed line shows E/N, calculated using B splines, for $N = 2$. Solid lines show E/N calculated by solving the nonlinear GP equation, Eq. (4), with the dipole-dependent scattering length. For comparison, a dotted line shows E/N for $N = 10$ calculated by solving the nonlinear GP equation, Eq. (4), with the bare scattering length, i.e., the cutoff radius b.

haviors for dipolar gases confined in elongated cigar-shaped and pancake-shaped traps.

Our variational many-body calculations for dipolar gases show that the region in configuration space where the metastable condensate exists is separated by an ''energy barrier'' from the region where bound many-body states exist. This energy barrier is familiar from variational treatments of atomic Bose-Einstein condensates with attractive interactions [28–30]. The existence of this barrier is crucial for our DMC calculations to converge to the metastable condensate state for sufficiently large D_*/a_{ho} and not to the clusterlike ground state. The dipolar gas collapses at the D_*/a_{ho} value for which the energy barrier vanishes. Our DMC calculations show that the condensate prior to collapse is only slightly elongated, which is consistent with our finding that the collapse is induced primarily by the negative value of a. After collapse, the particles assemble into a bound cluster, whose size is far smaller than the original condensate.

We now assess the validity of the GP equation for trapped dipolar Bose gases, which can be derived by performing a functional variation of the expectation value of the Hamiltonian given by Eq. (1), calculated with respect to a product wave function Ψ, $\Psi(\vec{r}_1, \cdots, \vec{r}_N) = \prod_{j=1}^{N} \chi(\vec{r}_j)$. For this procedure to be meaningful, the two-body interaction potential V, Eq. (2), has to be replaced by a pseudopotential V_{eff} [17]:

$$V_{\mathrm{eff}}(\vec{r}) = \frac{4\pi\hbar^2 a(d)}{m}\delta(\vec{r}) + d^2\frac{1-3\cos^2\theta}{r^3}, \qquad (3)$$

whose zero-energy T matrix, calculated in the first Born approximation, reproduces the full zero-energy T matrix of the model potential V, Eq. (2). The strength of the contact term of V_{eff} is not, as might be expected naively, given by the cutoff radius b but by the dipole-dependent s-wave scattering length $a(d)$. The GP equation for the single particle orbital $\chi(\vec{r})$ then reads

$$\left[\frac{-\hbar^2}{2m}\nabla^2 + \frac{1}{2}m\omega^2 r^2 + (N-1)\frac{4\pi\hbar^2 a(d)}{m}|\chi(\vec{r})|^2 + (N-1)d^2\int\frac{1-3\cos^2\theta}{|\vec{r}-\vec{r}'|^3}|\chi(\vec{r}')|^2 d^3\vec{r}'\right]\chi(\vec{r}) = \epsilon\chi(\vec{r}), \qquad (4)$$

where ϵ denotes the chemical potential. We solve the nonlocal equation (4) numerically by the steepest descent method. At each time step, the integration over the dipole potential is evaluated in momentum space with the aid of fast Fourier transforms [18].

The solid lines in Fig. 2 show the GP energies E/N per dipole for various N as a function of D_*/a_{ho}. Figure 2 shows excellent agreement between the GP and DMC energies (symbols) for all N considered. To illustrate that this agreement depends crucially on the value of the dipole-dependent s-wave scattering length a in the contact part of the pseudopotential V_{eff}, Eq. (3), a dotted line in Fig. 2 shows the GP energy per dipole for $N = 10$ obtained using the cutoff radius b instead of a. Figure 2 indicates that this simple description overestimates E/N severely when the dipole length D_* becomes comparable to and larger than the short-range length b.

Recently, an alternative, non-Hermitian, pseudopotential was proposed for two interacting dipoles [31]. This pseudopotential was applied, although unfortunately

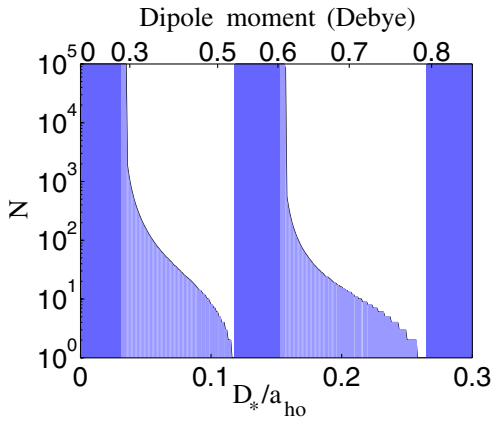

FIG. 3 (color online). Partial stability diagram for a dipolar condensate. The white regions depict parameters for which the gas is predicted to be mechanically unstable. Shaded areas are regions of stability, and dark shaded areas denote parameters that are expected to produce stable condensates even in free space. The top axis translates the dipole length D_* into a dipole moment, assuming a trap of frequency $\nu = 1$ kHz and a molecular mass 20 amu.

in an incorrect form, to extract properties of the dipolar gas [32]. Our results in this Letter strongly confirm that the original, simpler pseudopotential (3) advanced in Ref. [17] is actually quite accurate, and no extension is necessary at this point.

The dipole-dependent scattering length has important implications for the stability of a condensate, as shown in the N-vs-dipole stability diagram in Fig. 3. For concreteness, we have included an alternative horizontal axis, representing the dipole moment in Debye, assuming a trap of frequency $\nu = 1$ kHz and a molecular mass 20 amu, typical for light molecules. The shaded and white areas in Fig. 3 denote parameters for which the GP equation does and does not possess a solution, respectively. The dark shaded areas represent where the condensate is expected to be stable for any number of molecules, even in free space, as given by the criterion $a(d) > D_*/3$ [33]. Apart from these regions of "absolute" stability, the condensate for a fixed dipole moment will ultimately become unstable as the number of molecules is increased. Indeed, for certain values of dipole where $a(d)$ takes large, negative values (say, near $D_*/a_{\mathrm{ho}} = 0.27$), a condensate is not supported at all.

Alternatively, for fixed N, the condensate stability can be probed as a function of the dipole moment. This is likely a parameter more amenable to fine-tuning in the laboratory. In this case, an initially stable condensate will collapse after the dipole exceeds a certain value. There then follows a region of instability, followed by another region of stability as the dipole is made yet larger and the scattering length takes positive values. This alternating pattern of stable and unstable condensates continues beyond the two-and-a-half cycles we have shown in Fig. 3. This pattern is in contrast to the generally held view of polar condensate collapse, which would posit a single collapse when the dipole reaches a large critical value. Instead, there are many critical values, generated each time a new bound state is absorbed into the two-body potential. Because this collapse is largely s-wave dominated, the gas is much more nearly isotropic near the collapse point than has previously been reported.

In summary, we have tested, for the first time, the validity of the GP equation for describing Bose-Einstein condensates interacting via dipolar forces. We find that the GP equation works well as compared to essentially exact DMC methods, as long as the dependence of the s-wave scattering length on dipole moment is accounted for. Doing so, we predict a rich stability diagram for such a system, with alternating regions of stability and instability as the dipole moment is varied.

D. B. acknowledges financial support from the NSF under Grant No. PHY-0331529, S. R. from an anonymous fund and from the U.S.–Israel Educational Foundation (Fulbright Program), D. C. E. B. and J. L. B. from the DOE and the Keck Foundation.

[1] A. Griesmaier, J. Werner, S. Hensler, J. Stuhler, and T. Pfau, Phys. Rev. Lett. **94**, 160401 (2005).
[2] A. Griesmaier, J. Stuhler, and T. Pfau, Appl. Phys. B **82**, 211 (2006).
[3] S. Yi, L. You, and H. Pu, Phys. Rev. Lett. **93**, 040403 (2004).
[4] L. Santos and T. Pfau, Phys. Rev. Lett. **96**, 190404 (2006).
[5] J. Stuhler *et al.*, Phys. Rev. Lett. **95**, 150406 (2005).
[6] D. H. J. O'Dell, S. Giovanazzi, and G. Kuriziki, Phys. Rev. Lett. **90**, 110402 (2003).
[7] L. Santos, G. V. Shlyapnikov, and M. Lewenstein, Phys. Rev. Lett. **90**, 250403 (2003).
[8] S. Giovanazzi, D. O'Dell, and G. Kuriziki, Phys. Rev. Lett. **88**, 130402 (2002).
[9] K. Góral, L. Santos, and M. Lewenstein, Phys. Rev. Lett. **88**, 170406 (2002).
[10] B. Damski *et al.*, Phys. Rev. Lett. **90**, 110401 (2003).
[11] S. Y. T. van de Meerakker *et al.*, Phys. Rev. Lett. **94**, 023004 (2005).
[12] J. R. Bochinski, E. R. Hudson, H. J. Lewandowski, and J. Ye, Phys. Rev. A **70**, 043410 (2004).
[13] J. M. Sage, S. Sainis, T. Bergeman, and D. DeMille, Phys. Rev. Lett. **94**, 203001 (2005).
[14] D. Wang *et al.*, Eur. Phys. J. D **31**, 165 (2004).
[15] D. Egorov *et al.*, Eur. Phys. J. D **31**, 307 (2004).
[16] L. Santos, G. V. Shlyapnikov, P. Zoller, and M. Lewenstein, Phys. Rev. Lett. **85**, 1791 (2000); **88**, 139904 (2002).
[17] S. Yi and L. You, Phys. Rev. A **61**, 041604 (2000).
[18] K. Góral, K. Rzążewski, and T. Pfau, Phys. Rev. A **61**, 051601 (2000).
[19] J.-P. Martikainen, M. Mackie, and K.-A. Suominen, Phys. Rev. A **64**, 037601 (2001).
[20] S. Yi and L. You, Phys. Rev. A **63**, 053607 (2001).
[21] K. Góral and L. Santos, Phys. Rev. A **66**, 023613 (2002).
[22] S. Yi and L. You, Phys. Rev. A **66**, 013607 (2002).
[23] P. M. Lushnikov, Phys. Rev. A **66**, 051601 (2002).
[24] S. Ronen, D. C. E. Bortolotti, and J. L. Bohn, Phys. Rev. A **74**, 013623 (2006).
[25] S. Giovanazzi, A. Görlitz, and T. Pfau, Phys. Rev. Lett. **89**, 130401 (2002).
[26] B. L. Hammond, W. A. Lester, Jr., and P. J. Reynolds, *Monte Carlo Methods in Ab Initio Quantum Chemistry* (World Scientific, Singapore, 1994).
[27] S. Ronen, D. C. E. Bortolotti, D. Blume, and J. L. Bohn, Phys. Rev. A **74**, 033611 (2006).
[28] V. Pérez-García *et al.*, Phys. Rev. A **56**, 1424 (1997).
[29] H. T. C. Stoof, J. Stat. Phys. **87**, 1353 (1997).
[30] J. L. Bohn, B. D. Esry, and C. H. Greene, Phys. Rev. A **58**, 584 (1998).
[31] A. Derevianko, Phys. Rev. A **67**, 033607 (2003); **72**, 039901(E) (2005).
[32] S. Yi and L. You, Phys. Rev. Lett. **92**, 193201 (2004).
[33] C. Eberlein, S. Giovanazzi, and D. H. J. O'Dell, Phys. Rev. A **71**, 033618 (2005).